High-power CW >100 mW SOAs for active-passive integration

Student paper

Andrzej Jankowski[1], Stefanos Andreou [1], Steven Kleijn[1], Alonso Millan-Mejia[1], Pim Voorthuijzen[1], Thijs Buckers[1] and Luc Augustin[1]

[1]SMART Photonics, High Tech Campus 29, 5656 AE Eindhoven, The Netherlands
* luc.augustin@smartphotonics.nl

We report the first experimental results on our high-power continuous-wave (CW) multi-quantum-well amplifiers operating in 1550 nm range over a wide temperature span. Devices are compatible with active passive integration on an InP foundry platform. CW total output power of 100 mW at room temperature is recorded.

Keywords: *Ridge, high-power, SOA, amplifiers*

INTRODUCTION

Photonic integrated circuits' rapid market growth requires mature and reliable components fabricated with standardized industrial integration processes [1][2]. High-power devices at 1550 nm are the key components that find application in various modern systems, including lidar, telecommunication, and spectroscopy [3][4]. In this paper we present preliminary measurements and optical simulations of multi-quantum-well semiconductor optical amplifiers (SOA's) processed within SMART Photonics' InP foundry technology platform. The devices are designed for active-passive integration with other building blocks that are available within existing process design kits (PDKs).

DEVICE FABRICATION AND DESIGN

A general overview of the layer stack is presented in Fig. 1a. The designed layer stack is grown by metalorganic chemical vapor deposition (MOCVD) epitaxy. The stack is grown on an n-type InP substrate with a Q1.25 guiding layer positioned below an n-InP spacer layer, graded index separate confinement InGaAsP layers, and the quantum-well layer stack. The active region of the device is composed of compressively strained quantum wells that are separated with tensile strained barriers, followed by P-InP cladding and a P-InGaAs contact layer. A ridge structure is defined by lithography, followed by dry and wet etching. After wafer-thinning to 150 µm, devices are cleaved.

Offset quantum wells are utilized in the device design to lower the confinement factor and consequently increase the saturation output power of the semiconductor optical amplifier [5]. In Fig. 1b optical simulations of confinement factor (Γ) vs. thickness of the n-InP spacer layer results are presented. In the layer stack design, 100 nm of InP is chosen corresponding to ~1.8% of Γ in the active device region. Optical simulations of the ridge etch depth and width were performed to assure single-mode operation.

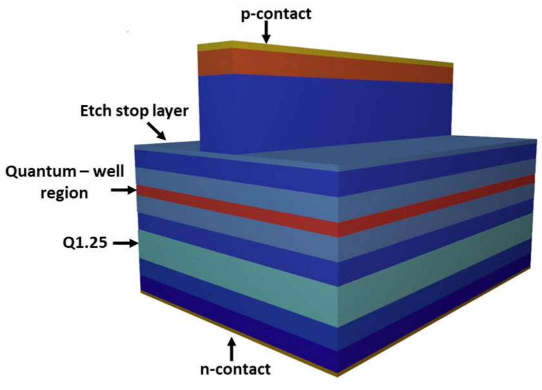

(a)

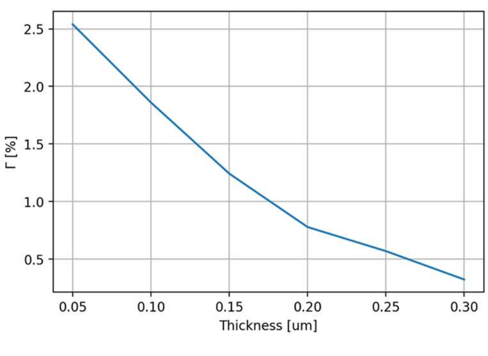

(b)

Fig. 1. Schematic overview of the layer stack (a) and (b) simulated optical confinement factor vs thickness of InP layer above optical waveguide core Q1.25.

RESULTS AND DISCUSSION

Firstly, Fabry Pérot (FP) lasers are characterised. Investigated devices were measured under continuous-wave (CW) and pulsed-mode operation. Cleaved and uncoated bars were directly placed in vacuum contact with the n-contact side on a copper mount, which was temperature-controlled by a thermoelectric cooler on top of a water-cooled heat sink. The output power is measured by collecting the output light an integrating sphere. The optical spectrum is measured using a cleaved single mode fiber and an optical spectrum analyser (OSA). Light-current and voltage-current measurements were performed as a function of temperature varying from 20 °C up to 50°C as long-wavelength InGaAsP devices are known to be strongly temperature-dependent [6].

The output power characteristics are presented in Fig. 2a, recorded under CW (solid-lines) and pulsed-mode (dashed-lines) operation, respectively. The maximum CW total output power (of both facets) of 100 mW is recorded for a device length of 2000 µm and ridge width of 4 µm at room temperature, with 86 mA of threshold current (I_{th}). Based on measured output power levels, the saturation power of an SOA should be higher due to higher facet reflectivity. The thermal roll-off of the output power is clearly visible. Additional power loss due to heat under CW operation shows at least 15% lower output powers at the same temperature point in comparison to pulsed-mode operation. Threshold current and threshold current density (J_{the}) increase over temperatures is depicted in Fig. 2b. The value of transparency threshold current density derived from linear fit of J_{th} and inverse cavity length is estimated to be 716 A/cm^2.

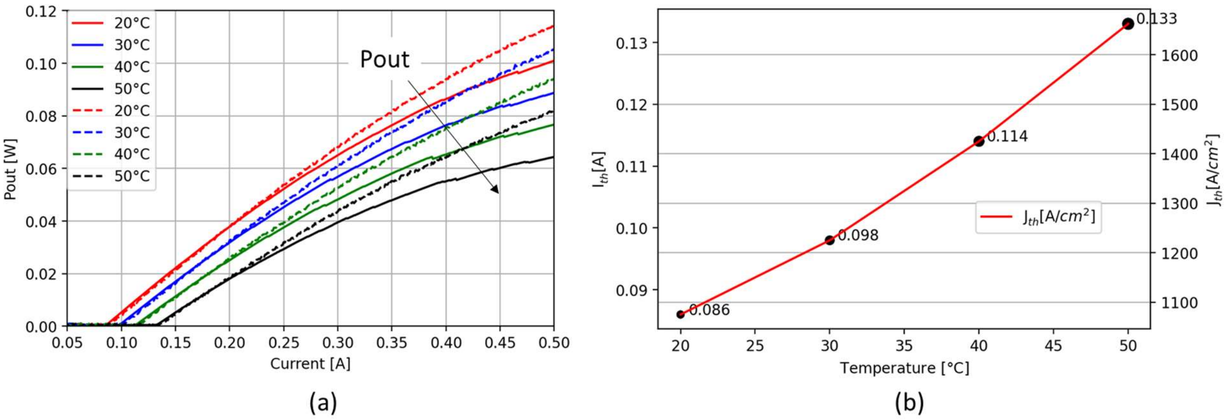

Fig. 2. (a) Measured light-current characteristics over temperature range between 20°C and 50°C, under CW operation (solid lines), pulsed-mode operation (dashed-lines) for the device length = 2000 µm and ridge width = 4 µm. (b) Recorded threshold current (I_{th}, left axis) and threshold current densities (J_{th}, right axis) vs. temperature.

Characteristic temperature measurements are presented in Fig. 3a and corresponding wall-plug efficiency in Fig. 3b. Recorded T_0 value of 68.5 K corresponds well with reported values in the literature [6], but it also suggests further improvements in thermal management are required.

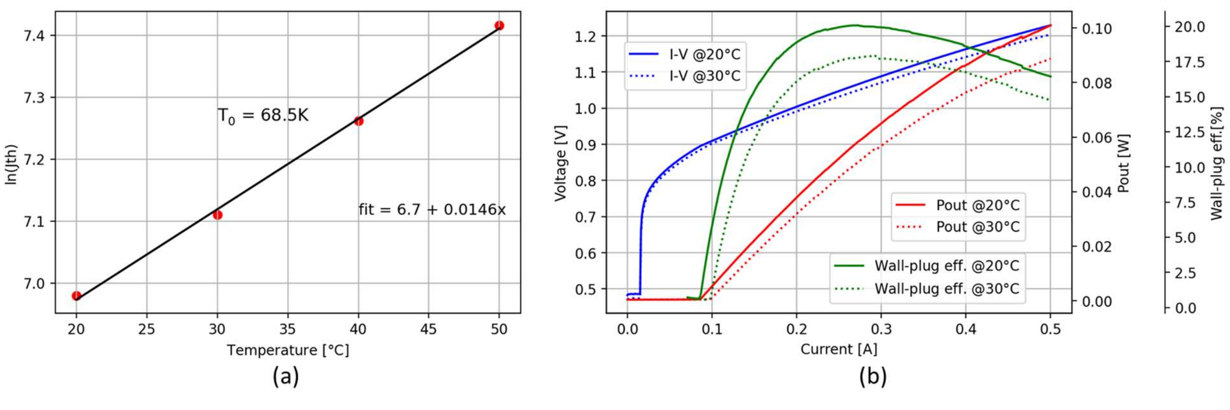

Fig. 3. (a) Characteristic temperature (T0) measurements and (b) measured characteristics of I-V, LI-V, and wall-plug efficiency at 20 °C and 30 °C. Device length = 2000 µm and ridge width = 4 µm.

We used an optical spectrum analyzer (OSA) to record the optical emission spectra operating around 1550nm. In Fig. 4, the optical spectra of the device are presented measured at 20 °C and 30 °C. The thermal red-shift of the wavelength emission is about 0.5 nm/K.

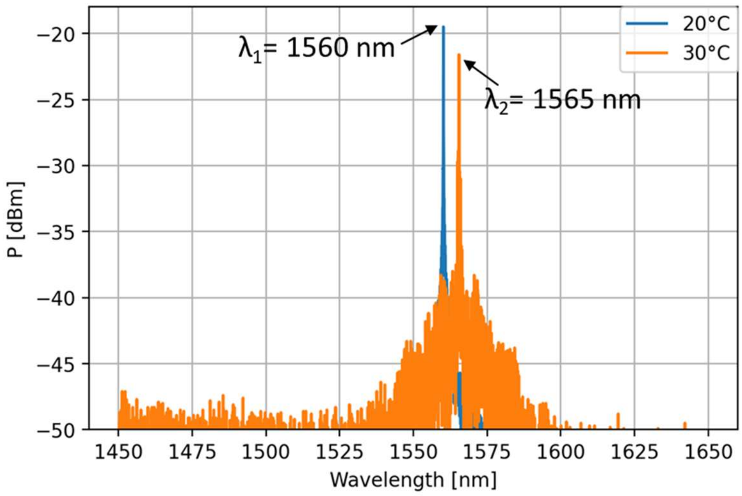

Fig. 4. Recorded optical spectrum at 20 °C for the device length of 2000 µm and 4 µm of ridge width.

SUMMARY

We have presented experimental measurement results of FP lasers fabricated on our InP foundry platform compatible with active-passive integration. Proposed devices show capability of >100 mW of total output power under CW operation and integration of SOAs with saturation powers at higher power levels due to higher facet reflectivity. Further analysis of SOAs using anti-reflective coated devices is planned.

As expected, strong temperature-dependent effects reducing the performance are observed. These influences are also confirmed in T_0 measurements, which suggest further improvements in thermal optimization are required to lower the thermal sensitivity of the devices. Introduction of Al-based Quantum wells will further improve the temperature behaviour.

References

[1] M. Smit, K. Williams, *Past, Present, and Future of InP-Based Photonic Integration* in APL Photonics 4, no. 5, 2019

[2] L. M. Augustin, R. Santos, *InP-Based Generic Foundry Platform for Photonic Integrated Circuits,* in IEEE Journal of Selected Topics in Quantum Electronics 24, no. 1, 2018

[3] D. Marpaung, J. Yao, *Integrated Microwave Photonics*, Nature Photonics 13, no. 2, 2019

[4] LiDAR application note, *Photonic integrated circuits for LiDAR*, SMART Photonics, 2021 (https://smartphotonics.hubspotpagebuilder.com/lidar)

[5] L. Nielsen, M. J. R. Heck, *Boosting the Output Power and Wall-Plug Efficiency of Lasers on a Generic InP Platform* in Integrated Optics: Devices, Materials, and Technologies XXV, SPIE, 2021

[6] J. Piprek, P. Abraham, *Self-Consistent Analysis of High-Temperature Effects on Strained-Layer Multiquantum-Well InGaAsP-InP Lasers* in IEEE Journal of Quantum Electronics 36, no. 3, 2000